Using Photogrammetric Methods for Mapping Geological Structures and Predicting Pitwall Kinematics at the Perseus Mine, Ayanfuri of Ghana*

[1]M. Affam and [1]P. E. Baffoe
[1]University of Mines and Technology, Tarkwa, Ghana

Affam, M. and Baffoe, P. E. (2020), "Using Photogrammetric Methods for Mapping Geological Structures and Predicting Pitwall Kinematics at the Perseus Mine, Ayanfuri of Ghana", *Ghana Journal of Technology,* Vol. 4, No. 2, pp. 66 - 79.

Abstract

This study introduces a novel approach of mapping geological structures in a mine for exploration and exploitation of the ore of that mine. In very unstable areas, the traditional method is usually inaccurate, time consuming and very risky. In this study a novel approach of photogrammetric principles was adopted for geological structural mapping at Perseus Mine. The geological structures of the pit walls were captured using Nikon D7000 camera and processed using SiroVision Version 5.1.11.0 software; and the kinematics analysis was done using Dips Version 5.103 software. In all, three individual mosaics were created using stereo models of the faces forming a composite image. The structural mapping was performed using SiroJoint a component of SiroVision. A total of 50 joints were mapped on the photographs. The orientation of the Dip and Dip directions were determined by plotting the mapped structures in Stereonet. This also helped to determine the areas of low to high concentrations using the Frictional Angle, Pit Slope, Daylight Envelope and the Critical Point. The strength of the intact rock was 54 MPa and as it falls in the range of 50-100 MPa it was rated 7. The space of discontinuity was 1.9 m which lies between 0.6 and 2.0 and was given a rating value of 15; condition of discontinuity of the face and was rated 25. The various rating values were put together giving the total rating value of 52 which helped to define the class and the description within which the rock was found. The cohesion of the rock mass lies between 200 and 300 kPa and the frictional angle between 25 and 30 degrees. SET 1 and SET 2 were kinematically stable but SET 3 is unstable, therefore sliding and hence failure is possible.

Keywords: SiroJoint, SirVision, Dip, Photogrammetric, Geological

1 Introduction

Generally, rock mass structural mappings as well as kinematic analysis are made to monitor and understand the behaviour of the rock mass in-situ. This normally helps geotechnical engineers to put measures in place to protect the workers in the pit and machinery from any eventual disaster.

Traditionally, geologists would stand in the open pit or underground mining face to map the rock structures which are visible onto a piece of paper. They would afterward collate the many bits of the information on paper and attempt to analyse the structures of the visible rocks; the process makes the work time consuming, dangerous and inefficient. One of the problems associated with 2D structural mapping is that there is bias in mapping structures which run perpendicular to the line of sight (Jami and Girard, 2001). It is also very risky and more dangerous to stand under the pit walls to map the geological structures; especially the freshly-blasted face and potentially unstable pit wall. The stability of the pit wall cannot be monitored by normal visual inspection.

A review of literature indicates that the traditional method takes time both in acquiring and processing the data (Tetteh, 2014). In the traditional method, fieldwork is dangerous, the possibility of rock-fall is high and missing potential areas could exist (Poropat, 2014). Due to the risk, biasness and time-consuming nature of geological mapping, the traditional method is problematic (Hoek and Bray, 1994). The advent of photogrammetric method of rock structural mapping is a promising technique to curb the potentially hazardous nature of traditional mapping in open pit mining (Little, 2005). This method applies sound geotechnical engineering practices, assisting mine design and general operating procedures. This method allows safe and economic mining of any ore within any rock mass and also assists mining operators in achieving their set goals of the mine development (Poropat 2014).

The behaviour of rock mass is a very important factor in the safety of mining and civil engineering projects (Romana, 1989). Rock falls are causes of major hazards in the mines and can have fatal consequences. Therefore being able to map the structures of a rock mass is crucial to understanding its potential behavior (John and Richard, 2015). This understanding can impact positively on safety and efficiency of mining or civil engineering projects thereby making geological mapping an important exercise (Hoek and Bray, 1994).

*Manuscript received August 20, 2019
Revised version accepted March 24, 2020

Mapping of the structure of a rock mass may be tedious if pit development plans, graph papers as well as series of strip maps are unavailable. It is unsafe to stand under freshly blasted inaccessible high walls and map unto a paper (Tetteh, 2014). Returning to the office, the geologist would collate the many bits of paper and attempt to analyse the structures which are visible. However, the mining and construction industries require a fast, reliable system of predicting and mapping of rock mass structure. Hence utilising digital mapping may be very useful.

The digital mapping of geological structure of rock mass provides the geologist and geotechnical engineer a better understanding of the ore bodies and extension potentials. These tools help them become more proactive by providing a complete view of data required to make decisions to mitigate risk and improve planning. This research work uses modern photo techniques to map geological structures and analyses the rock mass *in–situ*.

2. Resources and Methods Used

2.1 Study Area and Geological Settings

The study was conducted at Perseus Mining Limited, Ayanfuri of Ghana. The total area of their concession is approximately 122.46 km².

The mine concessions are located in the Central Region of Southern Ghana, on the eastern flanks of the highly prospective Ashanti Belt. The areas are located between 1°50′00″ west and 2°00′00″ west and 5°48′49″ north and 6°00′00″ north. The Project is approximately 57 km to the SW of the municipality of Obuasi and 195 km WNW of the capital Accra (Fig. 1) in Ghana, West Africa (Antwi, 2014).

2.1.2 Geological Settings

The area lies within the Precambrian Guinean Shield of West Africa. The geological formation hosts one of the most important auriferous rocks of metamorphosed and folded Birimian Supergroup (Kesse, 1985). The belt is dominated by a northeast-southwest trending structural feature which extends over 200 km along strike.

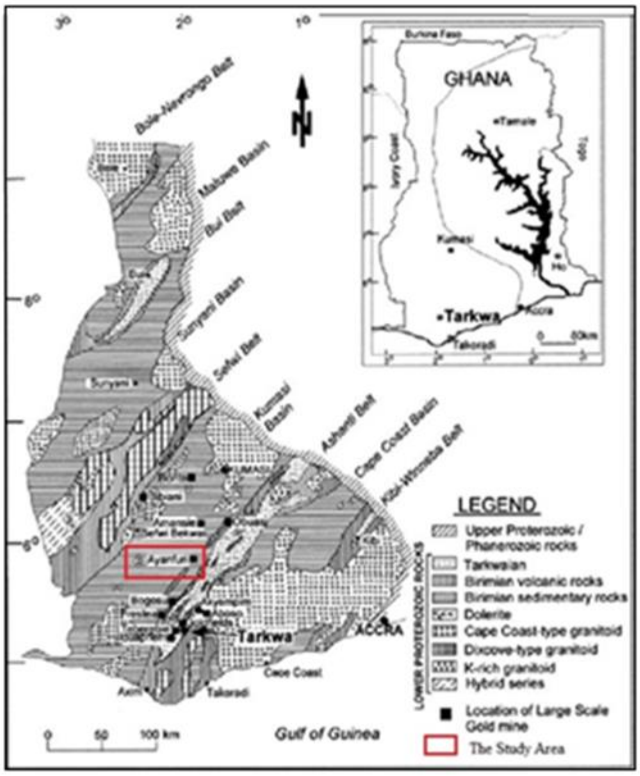

Fig. 1 Location of the Study Area (source: Kesse, 1985)

This structure is closely aligned with a faulted contact zone between the major lithological units: the metasedimentary and metavolcanic and some felsic to mafic intrusive. The metasedimentary sequence is described by Jami and Gerard (2001) as consisting of very thick beds of argillites and impure arenaceous and tufaceous sediments called schist, phyllites, greywakes, tuffs and slates. The metavolcanic sequence comprises of greenstones of metamorphosed basic lava and intrusive with complementary felsic lava and pyroclastic rocks. Manganiferous phyllites associated with hornstone and cherty beds are present in smaller quantities in upper horizons of the greenstones.

Generally, the most common structure at the mine is bedding (S_o). It is visible due to the grain size and colour variation, containing well preserved sedimentary structure, Bedding-cleavage intersections are uncommon. S_o/S_1 lineations plunge moderately northeast, while S_o/S_2 intersections have more diverse orientation. Five structural deformational events have been observed and according to recent studies they include:

(i) D_1-Event: Bedding parallel to shearing are non-uniformly distributed. More competent greywacke and volcanics remained unsheared.
(ii) D_2-Event: A fold thrust event, produced by moderate to steep dipping linear structures

with a NE strike within the Birimian and Tarkwaian sequence.

(iii) D_3-Event: This event caused the development of NE trending gentle folds with shallowly NW dipping axial planes. The event was local in nature and appeared to have very little influence on gold distribution.

(iv) D_4-Event: Developed a NNE to E tending fold which produced left-stepping flexures in bedding and earlier structures. These left-stepping structures are considered as the principal loci for gold lodes.

(v) D_5-Event: Principal Gold Event–induced a few meters to hundreds of meters of largely sinitral (left lateral) reactivation of the NE trending D_2 fault zones. This event is considered as the principal source of gold mineralisation of the Birimian systems.

2.1.1 Materials Used

An off-the-shelf single-lens reflex (SLR) digital camera, Nikon D7000, with the lens of focal length 60 mm was used; it mounted on a tripod before taking the photographs. The resolution can be achieved at a range between up to 2 000 m and is shown in Fig. 2.

Fig. 2 Nikon D7000 Camera

In addition, Schmidt Hammer was used in measuring the strength of the rock. In measuring the strength, there was the need to measure both the perpendicular and the horizontal strengths and the average taken as shown in Fig. 3.

Fig. 3 Schmidt Hammer

In order to georeference the mosaic of 3D photographic images of the rocks, a minimum of three (3) triangulated survey control points were required. These known control points can be any combination of surveyed camera positions (a camera on a tripod) or ground control points marked on to the actual rock surface. These points were surveyed using GPS receivers. There was a base station and rover receivers such as from Trimble incorporation with Geotaggers. These systems write GPS metadata onto the photographs as they are taken. The major advantages of this system are:

(i) The GPS data contained on the photographs file metadata.
(ii) Photographs can be rapidly taken hand-held, with no tripods necessary.
(iii) There is no requirement for external survey support.

There is no requirement to access the rock face to place control points, saving time and improving safety.

2.2 Methods Used

The methods employed in this paper are discussed in the following sections. The data was collected on the AG stage 3-East pit wall of Perseus Mining Ghana Limited. This was done using the camera to take photographs to map the various geological structures and also monitor its rate of movement to be able to analyse them.

2.2.1 Planning Reconnaissance and Mapping

The mapping task is first evaluated to ascertain the size of features to be mapped and the accuracy required; this helped to determine the lens to be used with a given camera and the geometry of the camera Ground Base. The camera positions were strategically selected such that the separation between the positions is approximately one sixth of the distance to the face being mapped. These were considered after a thorough site reconnaissance. In order for the mosaic of the 3D images to be accurately constructed, the camera positions were chosen so as to provide sufficient overlap to form the stereo model of the 3D images produced to build a mosaic with good coverage.

2.2.2 Field Procedures

In order to create accurately scaled 3D photographic images, three basic rules are applied as stipulated in photogrammetric ground measurements rules:

(i) The left and the right photographs of the same rock face must be taken to produce a stereopair;

(ii) The left and right photographs must have a baseline (distance between camera positions) at very roughly a ratio of 1:7 to the distance to the rock face; and

(iii) In order to mosaic 3D images together, adjacent stereopairs must overlap by around 30%.

2.2.3 Data Collection

To achieve the purpose of this task, primary data was obtained from the AG stage 3- East pit wall in the mine. The Dip and Dip Directions, the persistence, orientations as well as the displacement were determined through stereo photogrammetry. The data obtained were later transformed into the national grid where the Nothings, Eastings and Heights of each point on the wall were collected. Vital information was obtained from the Geotechnical Section of the mine with regards to the geology of the rock, the rock type, angle of repose, the strike and dip of the rock, the effect of the water table on the rock and some geological factors. These parameters aided in the investigation of the principal causes of displacement and how it influences failure of the pit wall.

2.2.4 Image Acquisition

The camera was set up on the tripod and aligned so that the chosen face is on or near the vertical centre line of the image. It was ensured that the camera and the tripod were levelled. The camera was then focused and the exposure station was constructed into the correct position. Relative Orientation facilities were used to determine camera orientation. Also, it was ensured that there was enough overlap in the two images to determine the camera orientation. The location of the camera was marked using a spray marker on the ground directly beneath the camera. It was ensured that the mark was vertical below the appropriate point of the camera – this is usually the intersection of the central axis of the lens and the mounting flange for the lens.

The instrument height of the camera on both the left control (LC) and the right control (RC) were recorded to be 1.5 m and 1.52 m respectively above the mark using the height from the mark to the position used for defining camera position (above) and was added to the reduced level (RL) of the pit.
The Second and third images were captured by repeating the procedure to the first pair remembering to ensure that the camera is levelled to start; the camera is then focused and that the exposure is 'good'; the camera position is marked with an appropriate reference on the ground and record the camera height above the mark.

A distance, '**S**' of 48 m was measured from the pit floor to the face of the pit wall using a laser. This was done perpendicular to the control point on the wall so that the left and right camera positions could be established. The Baseline distance '*B*' (m) is given by Equation (1):

$$B = \frac{s}{7}, \tag{1}$$

From Equation (1), since s is 48 m, $B = \frac{48}{7} = 6.8$ m. *B* is then divided by two in order to get an equal distance from the line of perpendicular to the left and right positions. Hence, $\frac{6.8}{2}$, was used to determine an equal distance of 3.4 m from the line of perpendicular to the left and right positions respectively. Fig. 4 shows how the images were taken.

2.2.5 Image Correction

The captured data was then downloaded from the camera in a raw format. They were then converted into TIFF images. For many cameras these can be 8 bit or 16 bit but for most applications 8 bit images are sufficient. Archive the raw images if required. The images are processed in order to correct for lens distortion.

These image corrections were done by applying image support and parameter of the lens that was used, selected from the menu of the software. The software then checked camera parameters such as camera model and lens focal length. It was ensured that these were chosen when the processes started. Once all the images have been corrected for lens distortion, the captured data is imported into the processing software called Sirovision as photographic images.

2.2.6 Georeferencing

To use the data effectively in the set of software packages selected for the work, the captured and corrected images were georeferenced in Sirovision software. The process provided a way whereby survey data, metadata, and attributes were integrated with the images. To fully complete the process, in order to georeference the mosaic of 3D images, a minimum of 3 triangulated control points were required. These known points can be any combination of surveyed camera positions (a camera on a tripod) or ground control points marked on to the actual rock surface. These points were surveyed using RTK GPS mode method, using base stations with rover receivers such as Trimble.

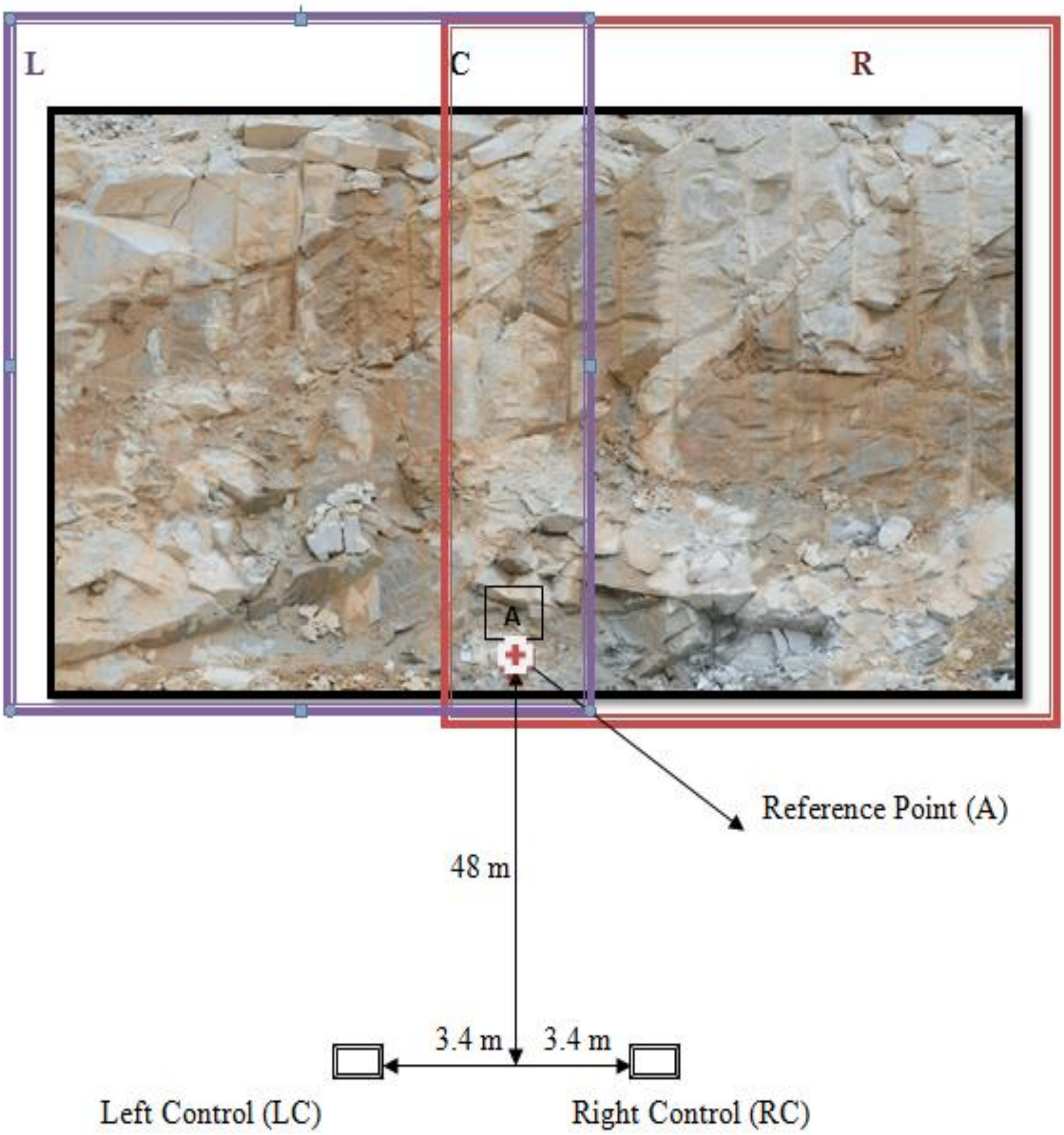

Fig. 4 Method of Obtaining Photographs for Sirovision

3 Results and Discussion

The results and discussion of the research are presented in the following sections.

3.1 Images Taken

The photographs taken are presented in Figs. 5 to 10. The images were taken in series, left, central and right. The first central image was taken containing the control point when stood on the left base station (FCL) and this is as seen in Fig. 5. Also, the image taken from the first central containing the control point when stood on the right base station (FCR) as in Fig. 6. The second left image containing the control point was taken when the camera was set on the left base station (SLL) as seen in Fig. 7. The third right image containing the control point was also taken when the camera was set on the left base station (TRL) as shown in Figs. 8-9**.** The second left image containing the control point was also taken when the camera was set on the right base station (SLR) as shown in Fig. 10**.** Then the **t**hird right image containing the control point was taken when the camera was set on the right control (TRR) as shown in Fig. 11.

Fig. 5 First Central Image Containing the Control Point when Stood on the Left Control (FCL)

Fig. 6 Second Left Image Containing the Control Point when Stood on the Left Control (SLL)

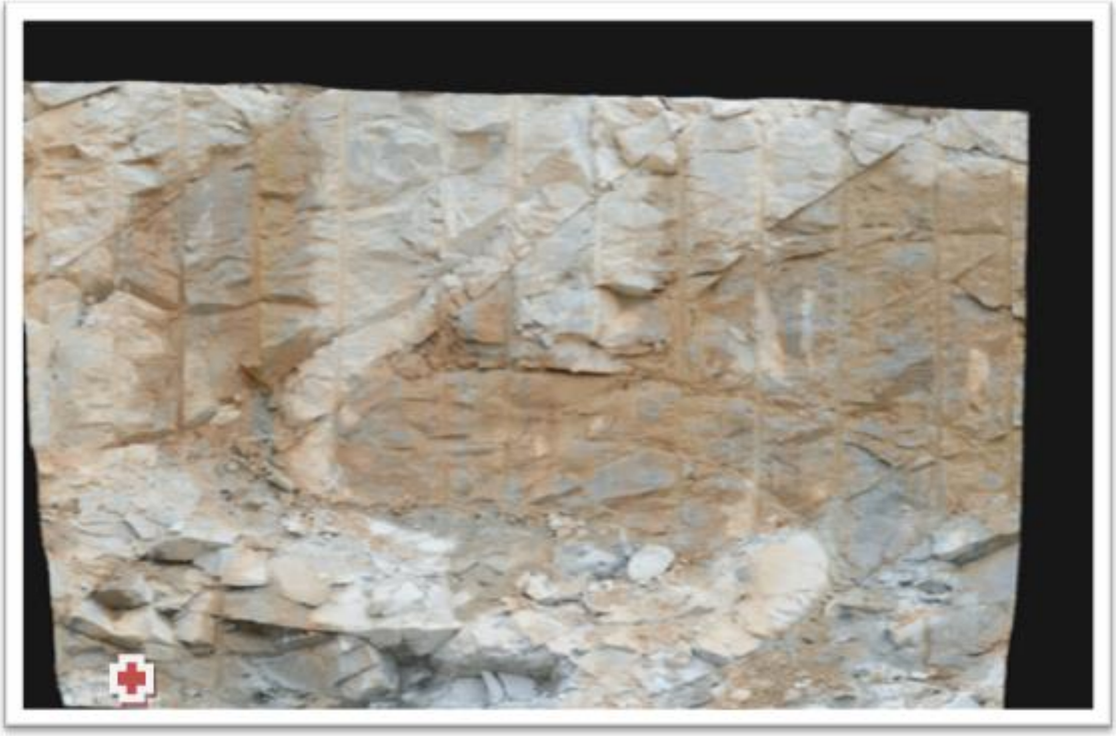

Fig. 7 Third Right Image Containing the Control Point when Stood on the Left Control (TRL)

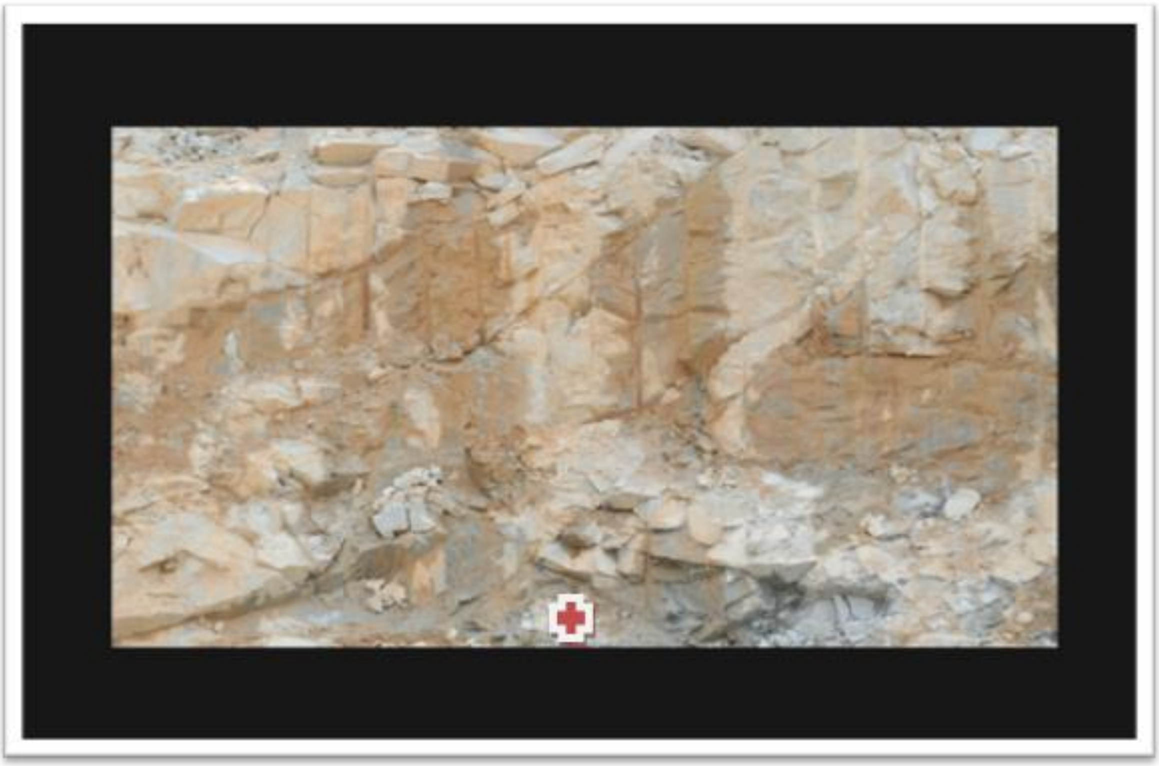

Fig. 8 First Central Image Containing the Control Point when Stood on the Right Control (FCR)

Fig. 9 Second Left Image Containing the Control Point when Stood on the Right Control (SLR)

Fig. 10 Third Right Image Containing the Control Point when Stood on the Right Control (TRR)

3.2 Mosaic

Mosaic is the pattern of putting pieces of pictures together to form one image. From Fig. 5 to Fig. 10, a mosaic was formed by combining FCL and FCR images, SLL and SLR images and TRL together with TRR images. In all, three (3) individual mosaics were formed. The three mosaics were combined to form a composite image as seen in Fig. 11.

3.3 Structural Mapping

Structural mapping was performed on the composite image using SiroJoint, a component of Sirovision software. A total of about 50 joints structures were mapped directly on the photograph. The ensuing figures below show the siroJoint mapped joints of the rock face. The arrows show the direction of the geological structures thus dip/dip directions of the mapped structures, letters A and B show the beginning and the ending of the mapped joints structure respectively as shown in Figs. 12 and 13.

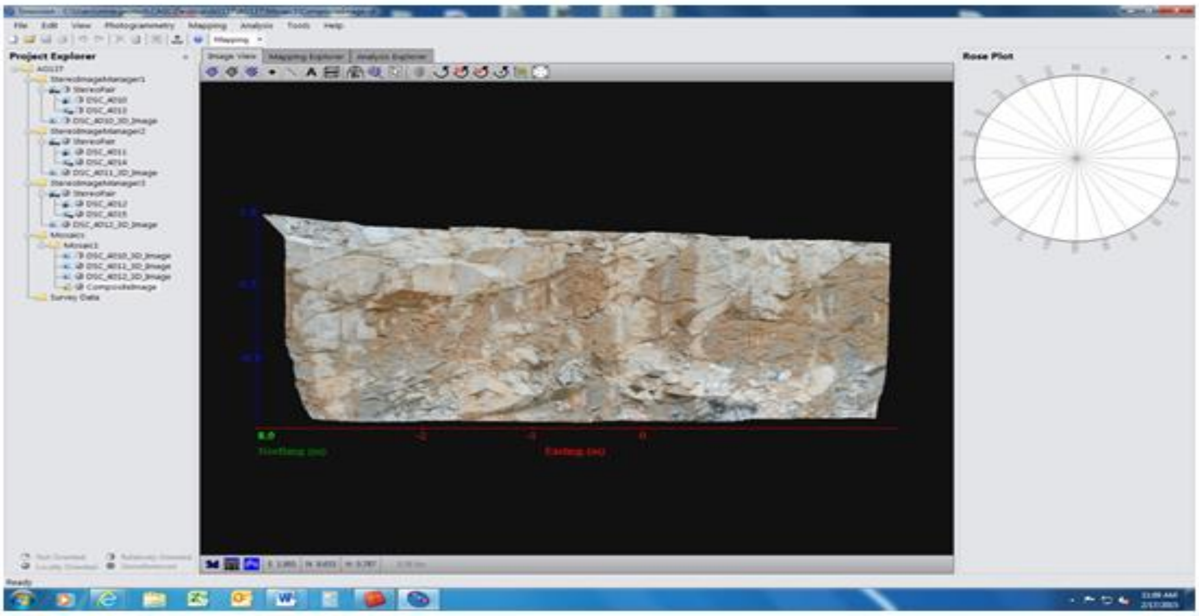

Fig. 11 Composite Image

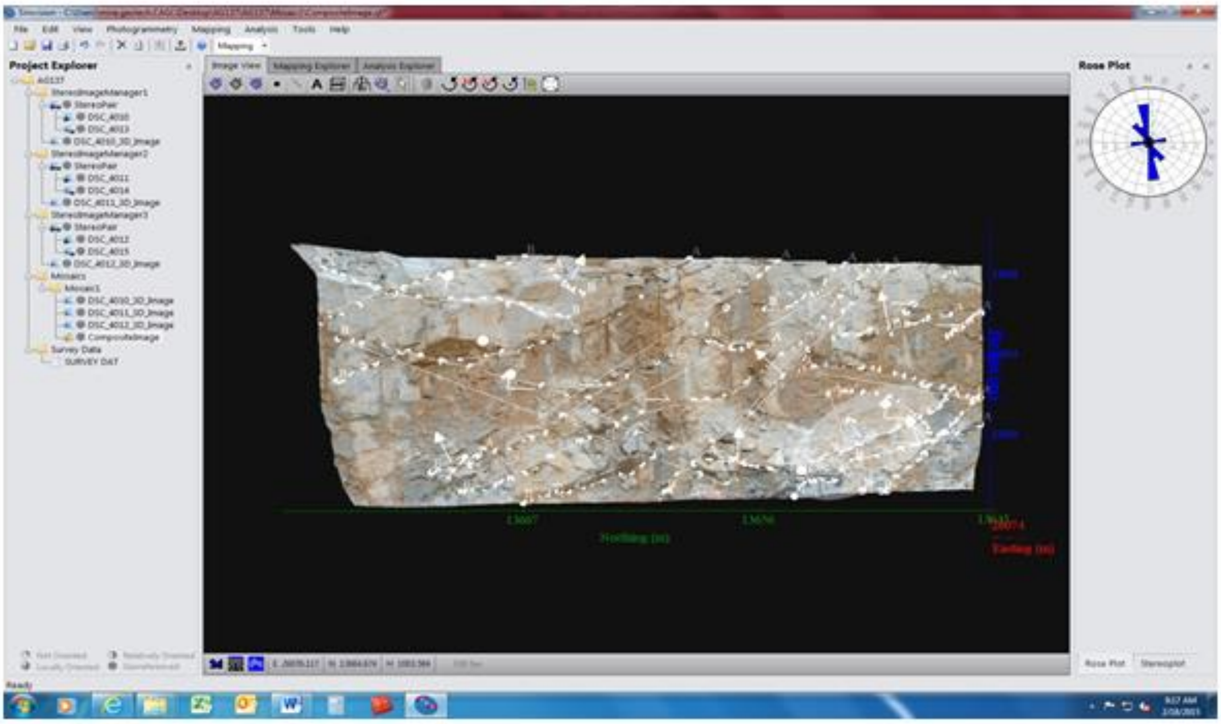

Fig. 12 Mapped Structures of the Rock Face using SiroJoint

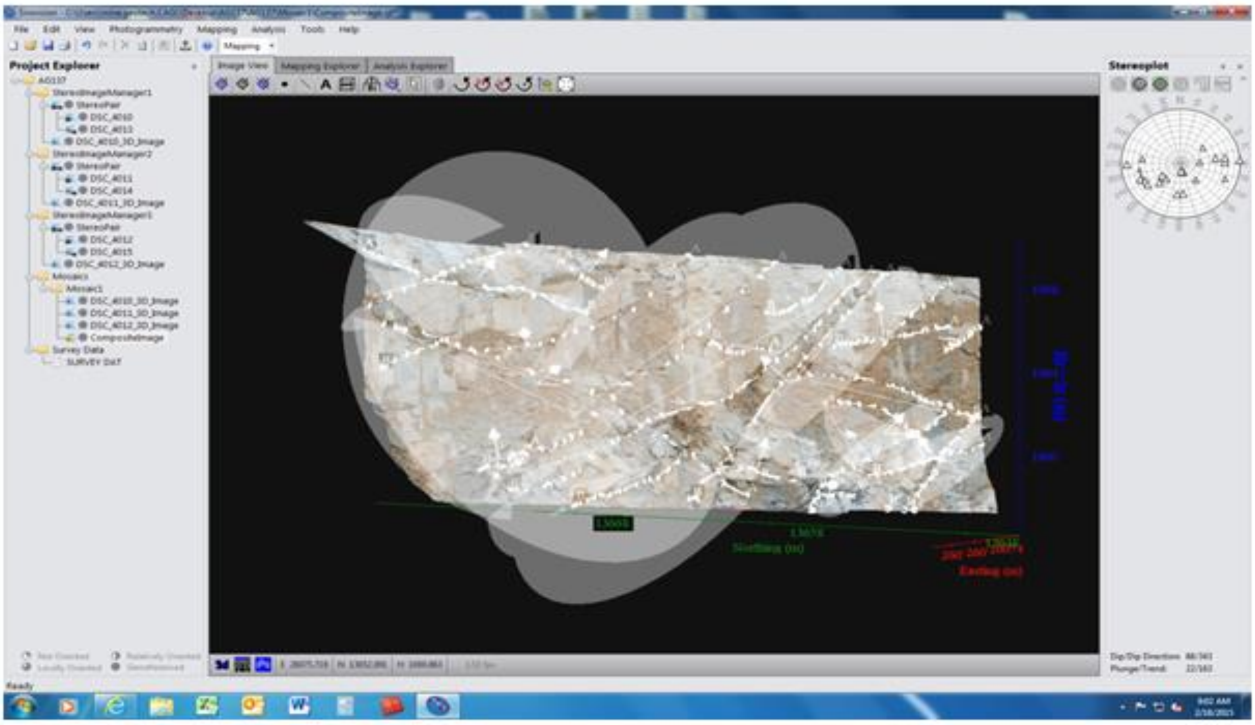

Fig. 13 Planes of the Mapped Surfaces Generated

After mapping the geological structures, the various dip/dip direction, the controls (Eastings, Northings and the Reduced Levels), and the type of structures mapped, orientations as well as the persistence were generated. The Fig. 14 shows the information on the composite image in the database structure.

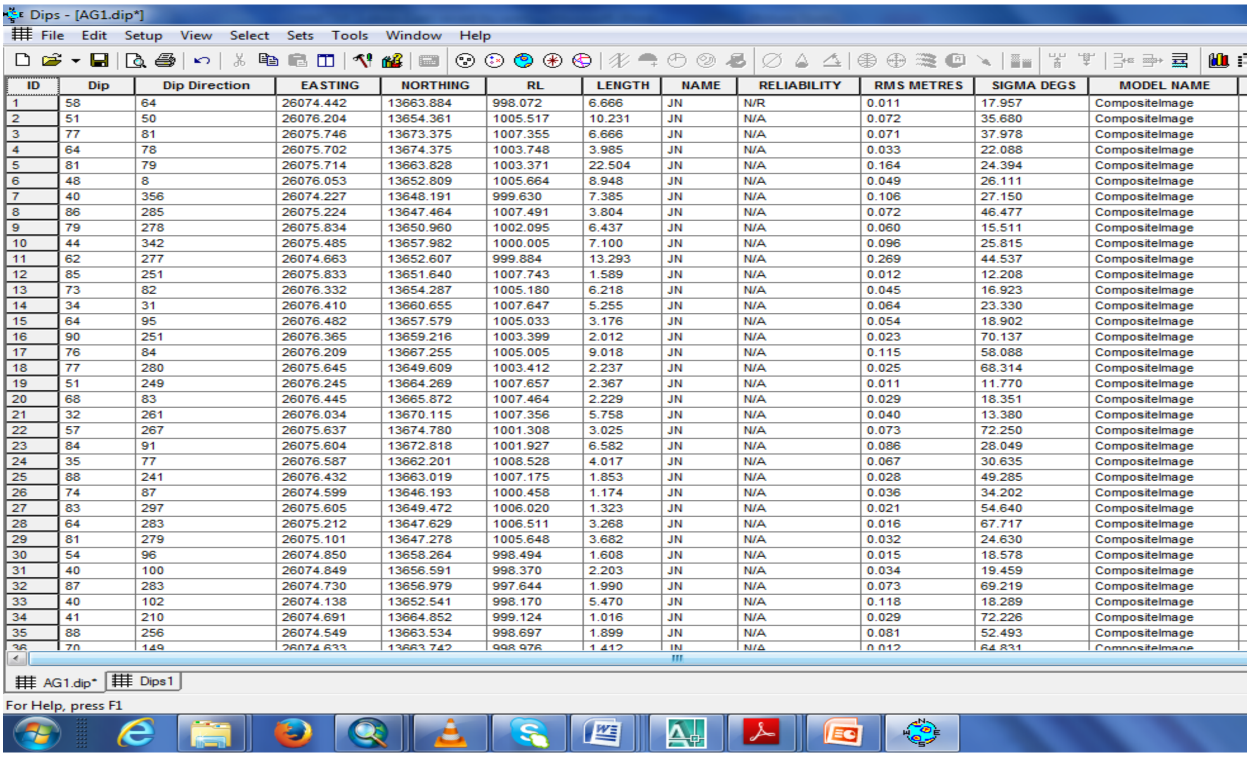

ID	Dip	Dip Direction	EASTING	NORTHING	RL	LENGTH	NAME	RELIABILITY	RMS METRES	SIGMA DEGS	MODEL NAME
1	58	64	26074.442	13663.884	998.072	6.666	JN	N/R	0.011	17.957	CompositeImage
2	51	50	26076.204	13654.361	1005.517	10.231	JN	N/A	0.072	35.680	CompositeImage
3	77	81	26075.746	13673.375	1007.355	6.666	JN	N/A	0.071	37.978	CompositeImage
4	64	78	26075.702	13674.375	1003.748	3.985	JN	N/A	0.033	22.088	CompositeImage
5	81	79	26075.714	13663.828	1003.371	22.504	JN	N/A	0.164	24.394	CompositeImage
6	48	8	26076.053	13652.809	1005.664	8.948	JN	N/A	0.049	26.111	CompositeImage
7	40	356	26074.227	13648.191	999.630	7.385	JN	N/A	0.106	27.150	CompositeImage
8	86	285	26075.224	13647.464	1007.491	3.804	JN	N/A	0.072	46.477	CompositeImage
9	79	278	26075.834	13650.960	1002.095	6.437	JN	N/A	0.060	15.511	CompositeImage
10	44	342	26075.485	13657.982	1000.005	7.100	JN	N/A	0.096	25.815	CompositeImage
11	62	277	26074.663	13652.607	999.884	13.293	JN	N/A	0.269	44.537	CompositeImage
12	85	251	26075.833	13651.640	1007.743	1.589	JN	N/A	0.012	12.208	CompositeImage
13	73	82	26076.332	13654.287	1005.180	6.218	JN	N/A	0.045	16.923	CompositeImage
14	34	31	26076.410	13660.655	1007.647	5.255	JN	N/A	0.064	23.330	CompositeImage
15	64	95	26076.482	13657.579	1005.033	3.176	JN	N/A	0.054	18.902	CompositeImage
16	90	251	26076.365	13659.216	1003.399	2.012	JN	N/A	0.023	70.137	CompositeImage
17	76	84	26076.209	13667.255	1005.005	9.018	JN	N/A	0.115	58.088	CompositeImage
18	77	280	26075.645	13649.609	1003.412	2.237	JN	N/A	0.025	68.314	CompositeImage
19	51	249	26076.245	13664.269	1007.657	2.367	JN	N/A	0.011	11.770	CompositeImage
20	68	83	26076.445	13665.872	1007.464	2.229	JN	N/A	0.029	18.351	CompositeImage
21	32	261	26076.034	13670.115	1007.356	5.758	JN	N/A	0.040	13.380	CompositeImage
22	57	267	26075.637	13674.780	1001.308	3.025	JN	N/A	0.073	72.250	CompositeImage
23	84	91	26075.604	13672.818	1001.927	6.582	JN	N/A	0.086	28.049	CompositeImage
24	35	77	26076.587	13662.201	1008.528	4.017	JN	N/A	0.067	30.635	CompositeImage
25	88	241	26076.432	13663.019	1007.175	1.853	JN	N/A	0.028	49.285	CompositeImage
26	74	87	26074.599	13646.193	1000.458	1.174	JN	N/A	0.036	34.202	CompositeImage
27	83	297	26075.605	13649.472	1006.020	1.323	JN	N/A	0.021	54.640	CompositeImage
28	64	283	26075.212	13647.629	1006.511	3.268	JN	N/A	0.016	67.717	CompositeImage
29	81	279	26075.101	13647.278	1005.648	3.682	JN	N/A	0.032	24.630	CompositeImage
30	54	96	26074.850	13658.264	998.494	1.608	JN	N/A	0.015	18.578	CompositeImage
31	40	100	26074.849	13656.591	998.370	2.203	JN	N/A	0.034	19.459	CompositeImage
32	87	283	26074.730	13656.979	997.644	1.990	JN	N/A	0.073	69.219	CompositeImage
33	40	102	26074.138	13652.541	998.170	5.470	JN	N/A	0.118	18.289	CompositeImage
34	41	210	26074.691	13664.852	999.124	1.016	JN	N/A	0.029	72.226	CompositeImage
35	88	256	26074.549	13663.534	998.697	1.899	JN	N/A	0.081	52.493	CompositeImage
36	70	149	26074.633	13663.742	998.976	1.412	JN	N/A	0.012	64.831	CompositeImage

Fig. 14 Data from 3D Models using Dips Software in a Structured Database

3.4 Kinematics Analysis

Kinematic analysis was done as a means of monitoring the stability of *the in-situ* rock mass that have structural flaws posing risk. These structures could fail and cause damage to workers and machinery. In kinematic analysis, Rock Mass Rating and Daylight Envelope are major factors that contribute to the rock mass analysis. Daylight Envelopes are used primarily in slope stability analysis work. It is kinematically feasible for any poles that plot within a Daylight Envelope to slide. To determine the stability of such poles, one must also consider the frictional strength, also known as the friction angle, thus the force of attraction between the rock mass in situ of the planes.

Rock Mass Rating system helps to determine the structural integrity of the rock mass. This system was established by Bieniawski (1976) and was updated in 1989. The updated version was used to analyse these results as tabulated below. The slope of the pit has a dip/direction of 53/270 respectively. This means that, any structure which daylight the slope angle and has frictional strength greater than that of the rock mass structure, sliding is kinematically possible for these planes hence is likely to fail.

3.5 Geological Structure and Rock Mass Strength

Rock mass failure occurs when the driving forces acting on a given body of material exceed the resisting forces within that body of material. In a freshly excavated slope, the force resisting failure can be attributed to the shear strength of the rock mass and geological structure. The driving force is primarily dependent on the unit weight of the rock mass, the geometry of the slope and the potential modes of failure. In soft rock, failure can propagate through the intact rock or along geological structure. In hard rock the path of minimum shear strength is predominantly along rock mass geological structure. It follows, therefore, that mine operators must identify the relevant modes of failure (the sources and magnitudes of the potential driving forces), and also determine and quantify the shear strength and other forms of resisting forces pertinent to that rock mass and mode of failure.

Table 1 Rock Mass Rating System Extract from Bieniawski (1989)

	PARAMETER	**RANGE OF VALUES**
1	Strength of intact rock material (54 MPa)	50-100 MPa
	Rating	7
2	Space of discontinuity (1.19 m)	0.6-2.0 m
	Rating	15
3	Condition of discontinuity	Slightly rough surfaces, Separation less than 1 mm. Slightly weathered walls
	Rating	25
4	Ground water	Damp
	Rating	10
5	**Rating Adjustment for Discontnuity Orientation**	**-5**
	Total Rating Value	**52**
Rock Mass Classes Determined From Total Rating		
Rating		41-60
Class number		III
Description		Fair rock
Meaning of Rock Classes		
Class number		III
Cohesion of rock mass (kPa)		200-300
Friction angle of rock mass (Degree)		25-35

From the table above, it can be seen that the friction angle of the rock mass (degrees) lies between 25 and 35 degrees. This means that any value from 25º to 35º can be used. With this, 35º was used as the frictional strength of the rock mass and was plotted as seen in the figures below. The slope of the pit has a dip/dip direction of 53/270 respectively. This was also plotted in the Stereonet or Dips as seen in Fig. 15 and Fig.16.

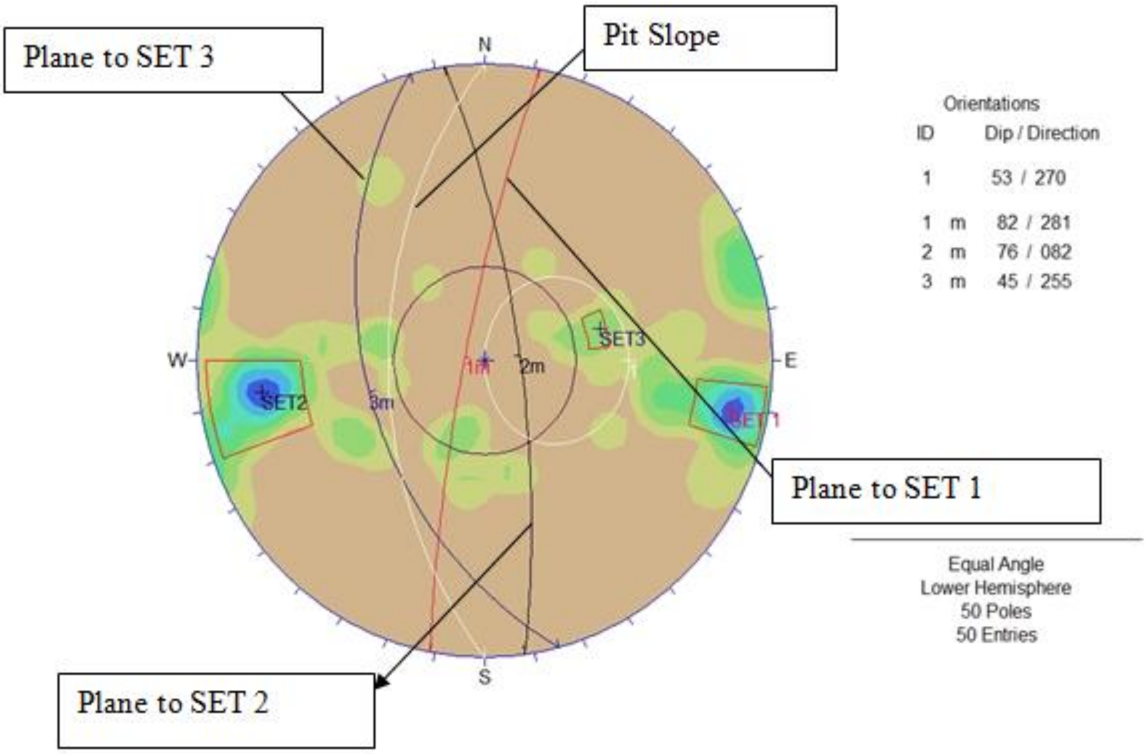

Fig. 15 Dip Values and Dip Directions of Mapped Structures Plotted in Stereonet Showing the Orientations of the Three (3) Sets

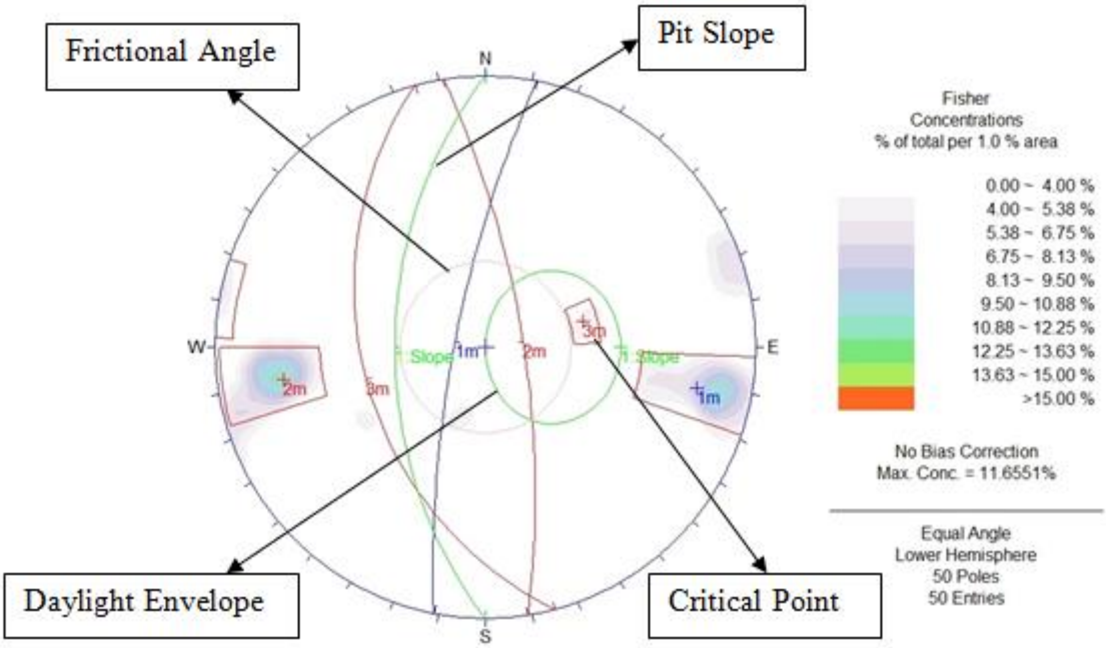

Fig. 16 Dip Values and Dip Directions of Mapped Structures Plotted in Stereonet Showing the Concentrations from Low to High Concentrated Area

3.6 Discussion

From the table, it can be seen that the strength of intact rock material has a value of 54 MPa, which falls in the rage of 50-100 Mpa, hence giving a rating of 7. The space of discontinuity is 1.19 m and lies between 0.6 and 2.0 m, giving a rating value of 15. This indicates condition of discontinuity of the face of the rock mass and is slightly rough surfaces. The separation is less than 1 mm and also the walls are slightly weathered. This has a rating of 25. The general water condition of the rocks in the area is damp from Table 1, giving a rating value of 10. The various rating values were put together giving a total rating value of 52. This rated value was used to define the class and the description within which the rock is found.

It has been shown that the rocks have a class of III with the description being a fair rock. Cohesion of rock mass (kPa) lies between 200 and 300 and the frictional angle of rock mass (Degree), was between 25 and 35 degrees.

In all, there are three (3) joint sets. Fig. 15 shows the orientation of the three sets whilst Fig. 16 depicts the fisher concentrations in percentage (%) of total per 1% area, with a maximum concentration of 11.6551%. SET 1, SET 2 and SET 3 with their orientations or planes are shown in Fig. 15. The area within the Daylight envelope, from Fig. 16 contains the poles to planes which have dip vectors outside the slope (i.e. sliding is kinematically possible for these planes). The daylight envelope represents all planes which can theoretically daylight from a given slope. In practice, planes which have a similar dip direction to the slope plane are more likely to fail.

SETS 1 and 2 though, are high in concentration of the joint structures but are kinematically stable. This is because, they are neither found within the friction circle nor the daylight envelope. Thus, for poles that plot inside the daylight envelope, but outside the friction circle, sliding is possible, hence SET 3. This is found inside the daylight envelope, but outside the friction circle. This means that, failure is likely to occur and the type of failure that can occur is planer failure. This is because, the failure will occur along the plane of the pit

4 Conclusions

Geological structural mapping and monitoring using the traditional method is very tedious, time consuming and dangerous. All these shortcomings associated with traditional method make the use of the Digital Mapping relatively safer and more convenient, effective and efficiently.

Sirovision software package has been used to map the 3D images of geological structures to determine the potential for toppling, wedge and planar failures through kinematic analysis. The designed size, shape and orientation of open pit excavations relative to the geological structure need to be recognised as a major factor controlling the number, size and shape of potentially unstable blocks that may form within the pit walls.

The structural mapping was performed using SiroJoint, a component of Sirovision; a total of 50 joints were mapped on the photographs. The orientation of the Dip and Dip directions were determined by plotting the mapped structures in Stereonet. This also helped to determine the areas of low to high concentrations using the Frictional Angle, Pit Slope, Daylight Envelope and the Critical Point. The strength of the intact rock was 54 MPa and it falls in the range of 50-100 MPa hence rate 7. The space of discontinuity was 1.9 m which lies between 0.6-2.0 and was given a rating the value of 15 condition of discontinuity of the face thus slightly weathered and rated 25. The various rating values were put together giving the total rating value of 52 which helped to define the class and the description within which the rock was found. The cohesion of the rock mass lies between 200-300 kPa and the frictional angle between 25-30 degrees. SET 1 and 2 were kinematically stable but SET 3 is unstable therefore sliding and hence failure is possible.

It is recommended that, all mining and civil engineering industries should adopt this modern method of mapping which is fast, safe and more efficient method for mapping and monitoring.
It is also recommended that, the mosaic of the whole mine should be generated for effective mine design and planning.

References

Antwi, M. (2014), “Pit Wall Monitoring at Perseus Mining Ghana Limited, Ayanfuri: A Case Study", *Unpublished BSc. Project Report,* University of Mines and Technology, Tarkwa, pp. 19-23.

Bieniawski, E. (1976), “Rock Mass Rating”, *www.globalmining.com*, Accessed: February 18, 2015.

Hoek, E. and Bray, J. W. (1994), *Rock Slope Engineering*, Chapman and Hall Publishers, UK, 560 pp.

Jami, M. and Girard, P. E. (2001), “Assessing and Monitoring Open Pit Mine High Walls”, *National Institute for Occupational Safety and Health Handbook*, 3rd Edition, Vol. 5, Montgomery Press, Spokane, USA, pp. 2-9.

John, W. B. and Richard, J. L. (2015), *Basic Geological Mapping*, John Wiley and Sons

Publishers, 4th Edition, West Sussex, England, 198 pp.
Kesse, G. O. (1985), *The Mineral and Rock Resources of Ghana*, A. A. Balkema Publishers, Rotterdam, 610 pp.
Little, M. J. (2005), "Understanding and Managing Kinematic Failure on the West Wall at Sandsloot Open Pit", *Proceedings of the Young Geotechnical Engineers Conference*, Swadini, South Africa, pp. 320-329.
Poropat, G. V. (2014), "New Methods for Measuring the Structure of Rock Mass" *Proceedings of Explo*. 2014, A. A. Balkema Publishers, Rotterdam, 230 pp.
Romana, H. (1989), "Geological Standard Index", *Bulletin of Engineering Geology and the Environment*, Vol. 54, pp. 8-19.
Tetteh, G. M (2014), "Mining Geology and Law", *Unpublished BSc Lecture Notes*, University of Mines and Technology, UMaT, Tarkwa, 76 pp.

Authors

M. Affam is currently an Associate Professor with the Department of Geological Engineering, University of Mines and Technology (UMaT), Tarkwa, Ghana. He holds PhD degree in Geological Engineering (Geotechnical option) from UMaT/ Queens University, Canada, MSc and BSc degrees from Kwame Nkrumah University of Science and Technology, Kumasi. Ghana. His specialty is in advances in geomechanics, foundation design and exploration techniques He doubles as a geotechnical consultant for several companies.

P. E Baffoe is a Senior Lecturer at the Department of Geomatic Engineering, University of Mines and Technology. He holds PhD degree (Geomatic Engineering) from University of Mines and Technology. His research interests include Monitoring, Prediction and Modelling of Noise Levels, Application of GIS in Environmental Issues, 3D Modelling, Digital Photogrammetry and Mine Surveying.